DYNAMIC ANALYSIS OF FUNCTIONALLY GRADED NANOCOMPOSITE BEAMS USING A MESH-FREE METHOD

Sayyidmousavi, A[1*], Foroutan, M[2], Fawaz, Z[3]

[1] Department of Applied Mathematics, Ryerson University,
Postdoctoral Fellow, Toronto, Canada
[2] Department of Mechanical Engineering, Razi University,
Associate Professor, Kermanshah, Iran
[3] Department of Aerospace Engineering, Ryerson University,
Professor, Toronto, Canada

* Corresponding author (asayyidmousavi@ryerson.ca)

ABSTRACT

Carbon NanoTubes (CNT's), due to their superior mechanical, thermal and electrical properties, have recently attracted numerous applications in different fields. In particular, their use as the reinforcing constituent for polymer matrix composites in place of conventional fibers has led to the emergence of a new generation of advanced composite materials. However, one problem with the application of CNT's as the reinforcing agent in polymers is the weak interfacial bonding between the CNT's and the matrix. This shortcoming can be alleviated through the use of Functionally Graded Materials (FGM's) in which material properties vary smoothly and continuously. This smooth variation of material properties is a major advantage of FGM's over conventional laminated composites where the sudden change in material properties across the interface causes delamination. In addition, in FGM's, the volume fractions of the constituents can be tailored for optimal performance of the structure. In this paper, the dynamic response of functionally graded nanocomposite beams under the action of a moving load as well as their free vibration on elastic foundations are investigated. Three different types of Carbon NanoTubes (CNT's) distributions in the polymer matrix material are studied; uniform distribution (UD), symmetrically functionally graded (SFG) distribution and unsymmetrically functionally graded (USFG) distribution. The analyses are carried out by a mesh-free method using the two-dimensional theory of elasticity. In mesh-free methods unlike the FEM, the material variation is captured at the integration points, which therefore results in more accurate results for functionally graded materials. After validation, the effects of CNT's distribution, the velocity and position of the moving load, slenderness ratios, boundary conditions and foundation stiffness on the dynamic behavior of the beam are examined. The results indicate the importance of the investigated effects from a design perspective. The current approach can serve as a benchmark against which other semi-analytical and numerical methods based on classical beam theories can be compared.

1 INTRODUCTION

Carbon NanoTubes (CNT's), due to their supreme mechanical, thermal and electrical properties, have recently attracted numerous applications in different fields. [1-3] In particular, their use as the reinforcing constituent for polymer matrix composites in place of conventional fibers has led to the emergence of a new generation of advanced composite materials. However, one problem with the application of CNT's as the reinforcing agent in polymers is the weak interfacial bonding between the CNT's and the matrix. This shortcoming can be alleviated through the use of Functionally Graded Materials (FGM's) in which material properties vary smoothly and continuously. [4] This smooth variation of material properties is a major advantage of FGM's over conventional laminated composites where the sudden change in material properties across the interface causes delamination. In

addition, in FGM's, the volume fractions of the constituents can be tailored for optimal performance of the structure.[5] It has been suggested by Shen (2009) [6] that using the concept of FGM, i.e., gradual distribution of CNT's in the matrix material can considerably improve the interfacial bonding strength between the CNT's and the matrix. Although a large amount of research has been dedicated to accurately obtaining the mechanical properties of Carbon NanoTube-Reinforced Composites (CNTRC's) [7-12], not as many studies have yet been conducted on the global response of CNTRC's to actual structural loading conditions in practical applications which is of course the ultimate purpose for the design and development of such materials. One example of the practical applications of such advanced composite materials are in FGM beam structures that are used to describe a lot of engineering problems and has application in geotechnics, road, railroad, marine engineering and bio-mechanics. In recent years, mesh free methods have been used as an efficient numerical method to solve different initial-boundary-value problems. Unlike the finite element method (FEM), in mesh-free methods the physical problem domain is modeled by only a set of scattered nodes without the need to be connected to form a closed polygon. The main advantage of mesh-free methods as compared to the FEM is the elimination of the mesh generation phase which can therefore save a considerable amount of time in the pre-processing phase. In addition, the computed stress by Mesh free methods result in smooth strain and stress fields without the need for any post-processing technique. As for functionally graded materials, since in mesh-free methods unlike the FEM, the material variation is captured at the integration points, fewer nodes will be required in the analysis of the problem for the same level of accuracy [5]. Different mesh-free methods have so far been proposed. Examples are the Diffuse Element Method (DEM) [13], the Element-Free Galerkin (EFG) method [14], the Hp-Clouds method [15], the Reproducing Kernel Particle Method (RKPM) [16], the Partition of Unity Finite Element Method (PUFEM) [17], and the Meshless Local Petrov-Galerkin (MLPG) method [18]. One of the most frequently used mesh-free methods in the analysis of solid mechanic problems is the Element Free Galerkin (EFG) method which utilizes the moving least square (MLS) shape functions. The main challenge in this method is the imposition of the essential boundary conditions due to the absence of the Kronecker delta property of the MLS shape function. To overcome this problem, the EFG method utilizes the Lagrange Multipliers Scheme for the imposition of the essential boundary conditions. However, this will be at the cost of increasing the number of degrees of freedom and resulting in a non-positive definite system matrix. In order to circumvent the afore-mentioned issue, in the present paper, the transformation technique [19] is used to impose the essential boundary conditions. In this technique, after the correction of the mesh-free shape functions, the essential boundary conditions are imposed as in the FEM causing the number of the degrees of freedom to remain unchanged. The bulk of the works in the literature are based on the assumptions of beam theories; mostly Euler-Bernoulli and Timoshenko. However, beam is a three-dimensional structure and although Timoshenko theory is an improvement on the Euler Bernoulli theory, the assumptions of the beam theories may not accurately represent the actual response of the structure. [20]. The object of the present work is to study the dynamic response of functionally graded nanocomposite beams under the action of a moving load as well as their free vibration on elastic foundations. In addition to the practical applications of the problem under consideration, the distinctive features of the current work are the use of a meshless method considering the afore-mentioned advantages and the two dimensional elasticity solution which can give a more realistic representation of the structures compared to beam theories especially as the aspect ratio of the beam increases. The FG beam in this study is reinforced by randomly oriented SWCNT's. It is assumed that the material properties vary in the thickness direction and are approximated using the Mori-Tanaka method [21]. In the mesh-free method, the moving least square (MLS) shape functions are implemented to approximate the displacement field. After validation, the effects of CNT's distribution, the velocity and position of the moving load, slenderness ratios, boundary conditions and foundation stiffness on the dynamic behavior of the beam are examined.

2   MATERIAL PROPERTIES

As the reinforcing constituent, CNT's are either aligned or randomly oriented in the isotropic matrix material. The effects of randomly oriented CNT's on the elastic properties of CNTRC's have been thoroughly investigated by Shi et al. [22]. They have concluded that despite the CNT's having transversely isotropic properties, when the CNT's are randomly oriented in the matrix, the composite material can be modeled as an isotropic material with its bulk K and shear modulus G defined as:

$$K = K_m + \frac{V_r(\delta_r - 3K_m\alpha_r)}{3(V_m + V_r\alpha_r)} \tag{1}$$

$$G = G_m + \frac{f_r(\eta_r - 2G_m\beta_r)}{3(V_m + V_r\beta_r)} \tag{2}$$

where K_m and G_m are the shear and bulk moduli of the matrix material, respectively. V_r and V_m denote the volume fractions of reinforcements and matrix, respectively and

$$\alpha_r = \frac{3(K_m + G_m) + k_r - l_r}{3(G_m + k_r)} \tag{3}$$

$$\beta_r = \frac{1}{5}\left\{\frac{4G_m + 2k_r + l_r}{3(G_m + k_r)} + \frac{4G_m}{G_m + p_r} + \frac{2[G_m(3k_m + G_m) + G_m(3K_m + 7G_m)]}{G_m(3K_m + G_m) + m_r(3K_m + 7G_m)}\right\} \tag{4}$$

$$\delta_r = \frac{1}{3}\left\{n_r + 2l_r + \frac{(2k_r + l_r)(3K_m + G_m - l_r)}{G_m + k_r}\right\} \tag{5}$$

$$\eta_r = \frac{1}{5}\left\{\frac{2}{3}(n_r - l_r) + \frac{8G_m p_r}{G_m + p_r} + \frac{8m_r G_m(3K_m + 4G_m)}{3K_m(m_r + G_m) + G_m(7m_r + G_m)} + \frac{2(k_r - l_r)(2G_m + l_r)}{3(G_m + k_r)}\right\} \tag{6}$$

k_r, l_r, m_r, n_r and p_r are the Hill's elastic moduli of the CNT's. The effective Young's Modulus E and Poisson's ratio υ are defined as:

$$E = \frac{9KG}{3K + G} \tag{7}$$

$$\upsilon = \frac{3K - 2G}{6K + 2G} \tag{8}$$

The volume fractions of the reinforcement V_r and matrix V_m are related as:

$$V_r + V_m = 1 \tag{9}$$

Three different cases are investigated; uniform distribution (UD), symmetrically functionally graded (SFG) distribution and unsymmetrically functionally graded (USFG) distribution. The reinforcement volume fraction V_r for each case is defined as follows:

$$V_r = \frac{4|y|}{h}\widehat{V}_r \qquad SFG \tag{10}$$

$$V_r = (1 - \frac{2y}{h})\widehat{V}_r \qquad USFG \tag{11}$$

where

$$\widehat{V}_r = \frac{w_r}{w_r + (\frac{\rho_r}{\rho_m}) - (\frac{\rho_r}{\rho_m})w_r} \tag{12}$$

w_r is the mass fraction of reinforcement. ρ_r and ρ_m are the densities of reinforcement and matrix, respectively. The mass density of the composite is calculated using the rule of mixtures:

$$\rho = \rho_r V_r + \rho_m V_m \tag{13}$$

Figure 1 schematically shows the FG beam cross sections for the three different CNT's distribution types. Table 1 lists the material properties of the SWCNT's reinforcement predicted through replacement with an equivalent long fiber [23].
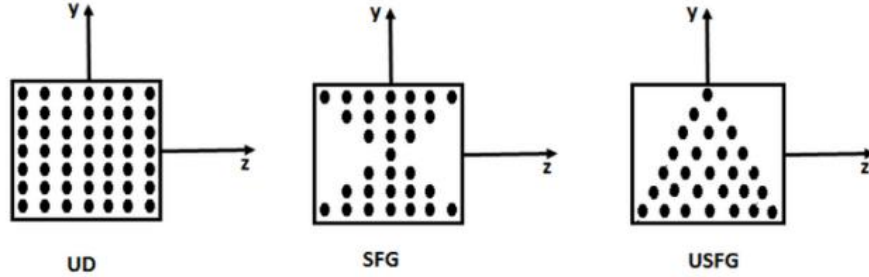

Figure 1: Schematic Representation of the CNT's distribution within the matrix material

Mechanical Property	
Longitudinal Modulus	649.12 (GPa)
Transverse Modulus	11.27 (GPa)
Longitudinal Shear Modulus	5.13 (GPa)
Poisson's ratio	0.284
Density	1400 (kg/m^3)

Table 1: Material properties of the SWCNT's reinforcement [23]

3 PROBLEM FORMULATION

The standard variational form of the equation of motion is expressed as follows:

$$\int_\Omega (\delta\varepsilon)^T \sigma.d\Omega - \int_\Gamma (\delta\mathbf{u})^T \mathbf{F}d\Gamma = -\int_\Omega (\delta\mathbf{u})^T \rho\ddot{\mathbf{u}}d\Omega \tag{14}$$

where σ, ε, $\mathbf{F}$, $\mathbf{u}$ and $\ddot{\mathbf{u}}$ represent stress, strain, surface traction, displacement and acceleration vectors respectively. Γ is a part of boundary of domain Ω on which traction $\mathbf{F}$ is applied. Stress and strain vectors are related through Hook's law:

$$\sigma = \mathbf{D}\varepsilon \tag{15}$$

In the present work, moving least square (MLS) shape functions introduced by Lancaster and Salkauskas [24] are used to approximate the displacement vector $\mathbf{u}$ at any point of interest using the nodes in the local support domain of that point. For a two dimensional problem:

$$\mathbf{u} = \varphi\hat{\mathbf{u}} \tag{16}$$

$\boldsymbol{\phi}$ and $\hat{\mathbf{u}}$ are the shape function matrix and the nodal values vector, respectively; n denotes the number of the nodes in the local support domain of the point of interest.

$$\boldsymbol{\varphi} = \begin{bmatrix} \phi_1 & 0 & ... & \phi_n & 0 \\ 0 & \phi_1 & ... & 0 & \phi_n \end{bmatrix} \tag{17}$$

$$\hat{\mathbf{u}} = \begin{bmatrix} u_1 & v_1 & ... & u_n & v_n \end{bmatrix}^T \tag{18}$$

The strain-displacement relation can be expressed in terms of the nodal values $\hat{\mathbf{u}}$ as follows:

$$\boldsymbol{\varepsilon} = \mathbf{B}\hat{\mathbf{u}} \tag{19}$$

where

$$\mathbf{B} = \begin{bmatrix} \dfrac{\partial \phi_1}{\partial x} & 0 & ... & \dfrac{\partial \phi_n}{\partial x} & 0 \\ 0 & \dfrac{\partial \phi_1}{\partial y} & ... & 0 & \dfrac{\partial \phi_n}{\partial y} \\ \dfrac{\partial \phi_1}{\partial y} & \dfrac{\partial \phi_1}{\partial x} & ... & \dfrac{\partial \phi_n}{\partial y} & \dfrac{\partial \phi_n}{\partial x} \end{bmatrix} \tag{20}$$

Substituting equations 15, 16 and 19 into the equation of motion (equation 14) yields:

$$\delta(\hat{\mathbf{u}})^T (\int_\Omega \mathbf{B}^T \mathbf{D} \mathbf{B} d\Omega)\hat{\mathbf{u}} - \delta(\hat{\mathbf{u}})^T \int_\Gamma \boldsymbol{\varphi}^T \mathbf{F} d\Gamma = -\delta(\hat{\mathbf{u}})^T (\int_\Omega \rho\boldsymbol{\varphi}^T \boldsymbol{\varphi} d\Omega)\ddot{\hat{\mathbf{u}}} \tag{21}$$

In the above-given equation the surface traction will be the reaction force of the elastic foundation which can be written in terms of nodal displacements:

$$\mathbf{F} = \mathbf{K_w}\boldsymbol{\varphi}\hat{\mathbf{u}} + \mathbf{K_P} \frac{\partial^2 \boldsymbol{\varphi}}{\partial x^2} \hat{\mathbf{u}} \tag{22}$$

where $\mathbf{K_W}$ and $\mathbf{K_P}$ are defined as follows:

$$\mathbf{K_W} = \begin{bmatrix} 0 & 0 \\ 0 & -k_w \end{bmatrix} \tag{23}$$

$$\mathbf{K_P} = \begin{bmatrix} 0 & 0 \\ 0 & k_p \end{bmatrix} \tag{24}$$

$\mathbf{K_W}$, known as the Winkler coefficient, is the spring stiffness of the foundation controlling the transverse deflection of the structure. $\mathbf{K_P}$, known as Pasternak coefficient, is the stiffness of a shear layer which accounts for the shear interactions on the vertical springs of the foundation. Figure 2 shows the geometry of a beam on Winkler-Pasternak foundation.
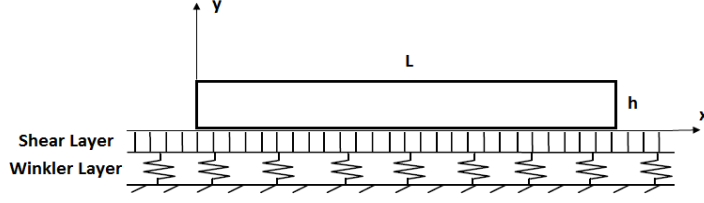
Figure 2: The geometry of the beam on a Winkler-Pasternak foundation

Rearranging equation 21 considering the fact that it should hold for any arbitrary $\delta(\hat{\mathbf{u}})^T$ leads to :

$$\mathbf{M}\ddot{\hat{\mathbf{U}}} + \mathbf{K}\hat{\mathbf{U}} = \mathbf{f} \tag{25}$$

where

$$\hat{\mathbf{U}} = \begin{bmatrix} u_1 & v_1 & ... & u_N & v_N \end{bmatrix}^T \tag{26}$$

$$\mathbf{K} = \int_\Omega \mathbf{B}^T \mathbf{D} \mathbf{B} d\Omega - \int_\Gamma \boldsymbol{\varphi}^T \mathbf{K}_\mathbf{W} \boldsymbol{\varphi} d\Gamma - \int_\Gamma \boldsymbol{\varphi}^T \mathbf{K}_\mathbf{P} \frac{\partial^2 \boldsymbol{\varphi}}{\partial x^2} d\Gamma \tag{27}$$

$$\mathbf{M} = \int_\Omega \rho \boldsymbol{\varphi}^T \boldsymbol{\varphi} d\Omega \qquad \mathbf{f} = \int_\Gamma \boldsymbol{\varphi}^T \mathbf{F} d\Gamma \tag{28}$$

N is the total number of nodes in the problem domain. For numerical integration, the problem domain is discretized into a set of background cells with gauss points inside each cell. Then global stiffness matrix $\mathbf{K}$ is obtained numerically by sweeping all gauss points inside Ω. Similarly global force vector $\mathbf{f}$ is formed numerically in the same manner but by sweeping all gauss points on Γ. Since the MLS shape functions do not possess the Kronecker delta property, the essential boundary conditions may not be directly imposed on the nodal vector $\hat{\mathbf{U}}$. To alleviate this problem, a transformation matrix is constructed which relates the real nodal displacement vector, $\mathbf{U}$ to $\hat{\mathbf{U}}$:

$$\mathbf{U} = \mathbf{T}\hat{\mathbf{U}} \tag{29}$$

where

$$\mathbf{T} = \begin{bmatrix} \phi_1(X_1) & 0 & \phi_2(X_1) & 0 & ... & \phi_N(X_1) & 0 \\ 0 & \phi_1(X_1) & 0 & \phi_2(X_1) & ... & 0 & \phi_N(X_1) \\ \vdots & \vdots & \vdots & \vdots & \vdots & \vdots & \vdots \\ \phi_1(X_N) & 0 & \phi_2(X_N) & 0 & ... & \phi_N(X_N) & 0 \\ 0 & \phi_1(X_N) & 0 & \phi_2(X_N) & ... & 0 & \phi_N(X_N) \end{bmatrix} \tag{30}$$

Using equation 25, equation 22 can be rewritten as:

$$\hat{\mathbf{M}}\ddot{\mathbf{U}} + \hat{\mathbf{K}}\mathbf{U} = \mathbf{0} \tag{31}$$

where

$$\hat{\mathbf{M}} = \mathbf{T}^{-T}\mathbf{M}\mathbf{T}^{-1} \qquad \hat{\mathbf{K}} = \mathbf{T}^{-T}\mathbf{K}\mathbf{T}^{-1} \qquad \hat{\mathbf{f}} = \mathbf{T}^{-T}\mathbf{f} \tag{32}$$

4 RESULTS AND DISCUSSIONS

4.1 Vibration Results

Table 2 lists the fundamental frequency parameters for simply supported beams on Winkler and Pasternak foundations compared with the exact solution obtained by Chen et al. [25]. The results are seen to be in very good agreement with the literature for both thin and thick beams.

Foundation Stiffness		L/h=120		L/h=15		L/h=5	
$\bar{k}w$	$\bar{k}p/\pi2$	Present	Exact [25]	Present	Exact [25]	Present	Exact [25]
0	0	3.142080	3.141417	3.130338	3.1302475	3.048003	3.0479950
	0.5	3.478399	3.476589	3.468103	3.4667123	3.395937	3.3945841
	1.0	3.738382	3.735859	3.728751	3.7265663	3.660169	3.6580220
	2.5	4.300635	4.296879	4.291623	4.2880929	4.221790	4.2183417
100	0	3.748612	3.748219	3.739004	3.7389477	3.670508	3.6705003
	0.5	3.961896	3.960669	3.952622	3.9516807	3.884874	3.8839762
	1.0	4.145417	4.143565	4.136320	4.1347188	4.067915	4.0663637
	2.5	4.585363	4.582264	4.576383	4.5734720	4.501957	4.4991384

Table 2: Fundamental frequency parameters for simply supported beams on Winkler and Pasternak foundations

In figure 3, the effect of the shear layer stiffness on the fundamental frequency of the structure is illustrated for two different slenderness ratios. It can be seen that for a given CNT's volume fraction and foundation stiffness, due to the symmetrically linear distribution of CNT's in the matrix material i.e., the existence of more CNT's in the high bending stress regions farther from the neutral axis, the SFG has the highest bending stiffness and consequently the highest natural frequency of all the three cases. Similarly, the unsymmetrical distribution of CNT's leads to the USFG distribution type having the lowest natural frequency. Also, increasing the foundation stiffness results in a more rigid structure thereby giving rise to the frequency of the vibration. From a design perspective, the vibrational response of a FG structure may be controlled in two ways; one way is through changing the distribution of the CNT's in the matrix material and the other way is by changing stiffness of the elastic foundation on which it is resting. However, as can be seen for thin beams, the latter approach seems more practical.
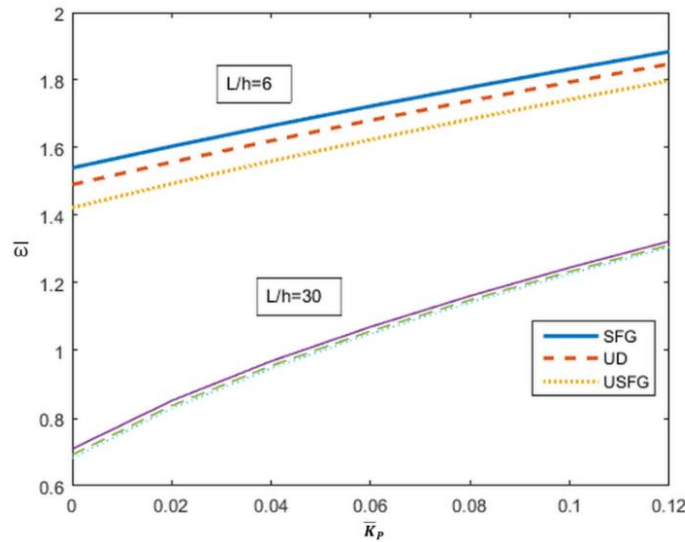

Figure 3: Effect of the shear layer stiffness on dimensionless fundamental frequency (C-C)

$$\widehat{V}_r = 0.26, \text{L/h=5}, \bar{k}w = 0.4$$

To study the effect of boundary conditions on the vibration of the SFG beams four combinations of free, simply supported, and clamped boundaries designated as C-C, C-S, S-S, C-F have been considered as shown in Figure 4.

The letters F, S, and C denote free, simply supported and clamped, respectively. It is seen that the fundamental frequency increases with greater geometric constraint in the following sequence (C-F, C-S, S-S, and C-C) which is due to the increase in the bending stiffness of the structure
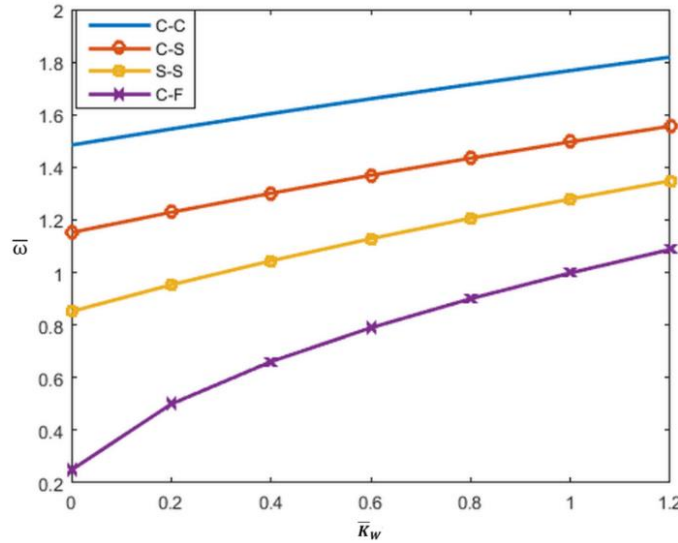

Figure 4: Effect of boundary conditions on dimensionless fundamental frequency

$$\widehat{V}_r = 0.26, \text{L/h=5}, \overline{k}p = 0.02$$

4.2 Moving Load Results

In this section, the dynamic behavior of the FG beam under the action of a moving load is studied. Figure 5 shows the deflection of the beam center for two different velocities during the free vibration i.e. after the load has exited the beam span. One can observe that the amplitude of the free vibration increases with the increase of the moving load velocity. It can also be seen that once the moving load has exited the beam span, the amplitude of the variations becomes stable due to the absence of damping. Another point worth mentioning is the phase difference between the three distribution types which increases with the elapse of time.
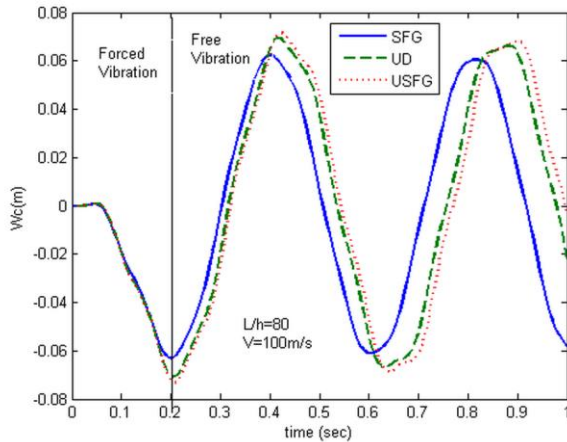

Fig. 5a: Deflection of the beam center
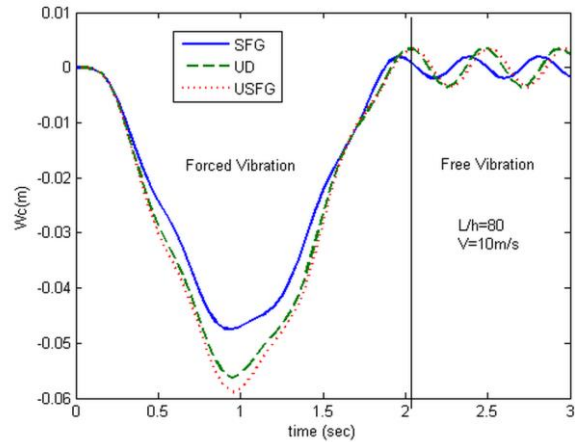(V=100m/s)

Fig. 5b: Deflection of the beam center
(V=10m/s)

Next, the effect of the velocity of the moving load is investigated. It can be seen in Figure 6 that increasing the velocity of the moving load delays the maximum deflection of the beam center. This delay increases with the

velocity of the moving load such that for the highest velocity, V=210 m/s, this maximum deflection occurs when the load has reached the very end of the beam span.
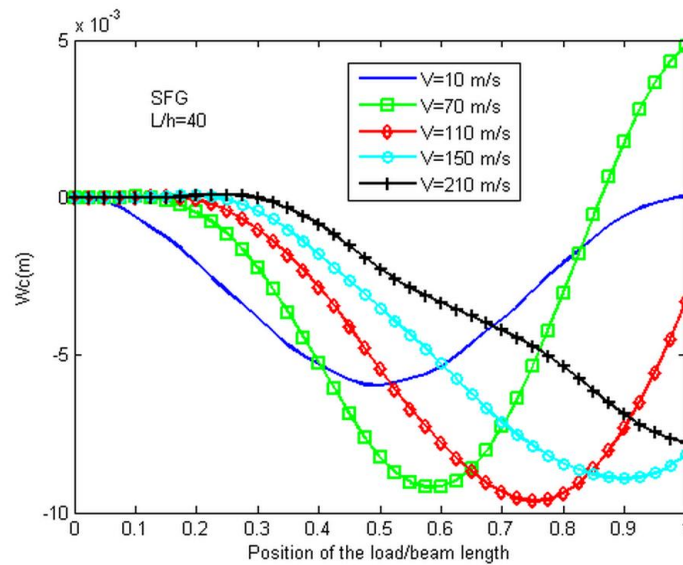

Fig. 6: Beam center deflections for different positions and velocity of the moving load

5   CONCLUSIONS

Some aspects of the dynamic behavior of functionally graded beams reinforced by randomly oriented SWCNT's are studied using a mesh-free method. Three different types of CNT's distributions in the polymer matrix material are investigated; uniform distribution (UD), symmetrically functionally graded (SFG) distribution and unsymmetrically functionally graded (USFG) distribution. The current two dimensional elasticity approach can serve as a benchmark against which other semi-analytical and numerical methods based on classical beam theories can be compared.

The symmetrical distribution of CNT's in the matrix material causes the SFG beam to have the highest bending stiffness and consequently the highest natural frequency of all the three cases. Similarly, the unsymmetrical distribution of CNT's, results in the USFG having the lowest natural frequency. Based on the same reasoning the SFG beam possesses the highest bending stiffness and thus the lowest deflection of the three cases. The rate of frequency increase due to foundation stiffness is seen to be higher for thin beams in comparison with thick beams.

As for the moving load analysis, it is observed that once the moving load has exited the beam span, the amplitude of the free vibration increases with the increase of the moving load velocity and that the phase difference between the three distribution types increases with time. A delay is observed between the maximum deflection of the beam center and the position of the load and is seen to increase with the moving load velocity. Also, the position of the beam where the maximum deflection of the beam takes place is seen to be travelling towards the end of the beam span as the velocity increases.

6   REFERENCES

[1]   H. Dai. "Carbon nanotubes: Opportunities and challenges". *Surface Science*, Vol. 500, No. 1-3, pp 218–241, 2007.

[2]   I. Kang, Y. Heung, J. Lee, J. Kim, R. Gollapudi, S. Subramaniam, S. Narasimhadevara, D. Hurd, G. Kirkera, V. Shanov, M. Schulz, D. Shi, J. Boerio, S. Mall and D. Ruggles-Wren. "Introduction to carbon nanotube and nanofiber smart materials". *Composites Part B*, Vol. 37, No. 6, pp 382–394, 2006.

[3]   K.T. Lau, C. Gu and D. Hui. "A critical review on nanotube and nanotube/nanoclay related polymer composite materials". *Composites Part B*, Vol. 37, No.6, pp 425–436, 2006.

[4] M.H. Yas and N. Samadi. "Free vibrations and buckling analysis of carbon nanotube-reinforced composite Timoshenko beams on elastic foundation". *International Journal of Pressure Vessels and Piping*, Vol. 98: pp 119-128, 2012.

[5] L.F. Qian and H.K. Ching. "Static and dynamic analysis of 2-D functionally graded elasticity by using meshless local petrov- galerkin method". *Journal of Chinese Institute of Engineers*, Vol. 27, No. 4, pp 491-503, 2011.

[6] H.S. Shen. "Nonlinear bending of functionally graded carbon nanotube reinforced composite plates in thermal environments". *Composite Structures*, Vol. 91, No. 1, pp 9–19, 2009.

[7] G.M. Odegard, T.S. Gates, K.E. Wise, C. Park and E.J. Siochi. "Constitutive modeling of nanotube-reinforced polymer composites". *Composite Science and Technology*, Vol. 63, No. 11, pp 1671–1687, 2003.

[8] N. Hu, H. Fukunaga, C. Lu, M. Kameyama and B. Yan. "Prediction of elastic properties of carbon nanotube reinforced composites". *Proceedings of the Royal Society A*, Vol. 461, pp 1685–1910, 2005.

[9] J.D. Fidelus, E. Wiesel, F.H. Gojny, K. Schulte and H.D. Wagner. "Thermo-mechanical properties of randomly oriented carbon/epoxy nanocomposites". *Composites Part A*, Vol. 36, No. 11, pp 1555–1561, 2005.

[10] P. Bonnet, D. Sireude, B. Garnier and O. Chauvet. "Thermal properties and percolation in carbon nanotube–polymer composites". *Journal of Applied Physics*, Vol. 91, No. 20, pp 2019–2030, 2007.

[11] Y. Han and J. Elliott. "Molecular dynamics simulations of the elastic properties of polymer/carbon nanotube composites". *Computational Materials Science*, Vol. 39, No. 2, pp 315–323, 2007.

[12] R. Zhu, E. Pan and A.K. Roy. "Molecular dynamics study of the stress–strain behavior of carbon-nanotube reinforced Epon 862 composites". *Materials Science and Engineering: A*, Vol. 447, No. 1-2, pp 51–57, 2007.

[13] B. Nayroles, G. Touzot and P. Villon. "Generalizing the finite element method: Diffuse approximation and diffuse elements". *Computational Mechanics*, Vol. 10, No. 5, pp 307-318, 1992.

[14] T. Belytschko, Y.Y. Lu and L. Gu. "Element-Free Galerkin Methods". *International Journal of Numerical Methods in Engineering*, Vol. 37, No. 2, pp 229-256, 1994.

[15] C.A. Duarte and J.T. Oden. "H-p Clouds − an hp Meshless Method". *Numerical Methods Partial Differential Equations*, Vol. 12, No. 1-4, pp 673-705, 1996.

[16] W.K. Liu, S. Jun and Y.F. Zhang. "Reproducing Kernel Particle Methods". *International Journal of Numerical Methods in Engineering*, Vol. 38, No. 10, pp 1081-1106, 1995.

[17] J.M. Melenk and I. Babuska. "The partition of Unity Finite Element Method: Basic theory and applications". *Computer. Methods in Applied Mechanics and Engineering*, Vol. 139, No. 1-4, pp 289-314, 1996.

[18] S.N. Atluri and T. Zhu. "The Meshless Local Petrov-Galerkin (MLPG) Approach for solving problems in elasto-statics". *Computational. Mechanics*, Vol. 25, No. 2, pp 169-179, 2000.

[19] R. Moradi-Dastjerdi, M. Foroutan and A. Pourasghar. "Dynamic analysis of functionally graded nanocomposite cylinders reinforced by carbon nanotube by a mesh-free method". *Materials and Design*, Vol. 44, pp 256-266, 2013.

[20] A. Labuschagne, N.F.J. VanRensburg and A.J. Van der Merwe. "Comparison of linear beam theories". *Mathematical and Computer Modelling*, Vol. 49, No. 1-2, pp 20-30, 2009.

[21] T. Mori and K. Tanaka. "Average stress in matrix and average elastic energy of materials with misfitting inclusions". *Acta Metallurgica*, Vol. 21(5): pp 571–574, 1973.

[22] D.L. Shi, X.Q. Feng, Y.Y. Huang, K.C. Hwang and H. Gao. "The effect of nanotube waviness and agglomeration on the elastic property of carbon nanotube reinforced composites". *Journal Engineering Materials and Technology*, Vol. 126, No. 3, pp 250–257, 2004.

[23] M.H. Yas and M. Heshmati. "Dynamic analysis of functionally graded nanocomposite beams reinforced by randomly oriented carbon nanotube under the action of moving load". *Applied Mathematical Modelling*, Vol. 36(4): pp 1371-1394, 2012.

[24] P. Lancaster and K. Salkauskas. "Surface generated by moving least squares methods". *Mathematics of Computation*, Vol. 37, No. 154, pp 141–58, 1981.

[25] W.Q. Chen, C.F. Lu and Z.G. Bian. "A mixed method for bending and free vibration of beams resting on a Pasternak elastic foundation*". Applied Mathematical Modelling*, Vol. 28, No. 10, pp 877-890, 2004.

.